2013

Electrochemical Investigation of a Microbial Solar Cell Reveals a Nonphotosynthetic Biocathode Catalyst

Sarah M. Strycharz-Glaven
U.S. Naval Research Laboratory, sarah.glaven@nrl.navy.mil

Richard H. Glaven
Nova Research, Inc.

Zheng Wang
U.S. Naval Research Laboratory

Jing Zhou
Nova Research, Inc.

Gary J. Vora
U.S. Naval Research Laboratory

See next page for additional authors

AEM
Journals.ASM.org

Electrochemical Investigation of a Microbial Solar Cell Reveals a Nonphotosynthetic Biocathode Catalyst

Sarah M. Strycharz-Glaven,[a] Richard H. Glaven,[b] Zheng Wang,[a] Jing Zhou,[c] Gary J. Vora,[a] Leonard M. Tender[a]

Center for Bio/Molecular Science and Engineering, U.S. Naval Research Laboratory, Washington, DC, USA[a]; Nova Research, Inc., Alexandria, Virginia, USA[b]; IBM Almaden Research Center, San Jose, California, USA[c]

Microbial solar cells (MSCs) are microbial fuel cells (MFCs) that generate their own oxidant and/or fuel through photosynthetic reactions. Here, we present electrochemical analyses and biofilm 16S rRNA gene profiling of biocathodes of sediment/seawater-based MSCs inoculated from the biocathode of a previously described sediment/seawater-based MSC. Electrochemical analyses indicate that for these second-generation MSC biocathodes, catalytic activity diminishes over time if illumination is provided during growth, whereas it remains relatively stable if growth occurs in the dark. For both illuminated and dark MSC biocathodes, cyclic voltammetry reveals a catalytic-current–potential dependency consistent with heterogeneous electron transfer mediated by an insoluble microbial redox cofactor, which was conserved following enrichment of the dark MSC biocathode using a three-electrode configuration. 16S rRNA gene profiling showed *Gammaproteobacteria*, most closely related to *Marinobacter* spp., predominated in the enriched biocathode. The enriched biocathode biofilm is easily cultured on graphite cathodes, forms a multimicrobe-thick biofilm (up to 8.2 μm), and does not lose catalytic activity after exchanges of the reactor medium. Moreover, the consortium can be grown on cathodes with only inorganic carbon provided as the carbon source, which may be exploited for proposed bioelectrochemical systems for electrosynthesis of organic carbon from carbon dioxide. These results support a scheme where two distinct communities of organisms develop within MSC biocathodes: one that is photosynthetically active and one that catalyzes reduction of O_2 by the cathode, where the former partially inhibits the latter. The relationship between the two communities must be further explored to fully realize the potential for MSC applications.

It has been hypothesized that microbial solar cells (MSCs) can continuously generate electricity from sunlight without additional oxidant or fuel, since the products of photosynthesis (e.g., oxygen and organic carbon) can be utilized as electrode reactants while the electrode products (e.g., inorganic carbon and water) can be utilized as photosynthetic reactants (1) (see Fig. S1 in the supplemental material). MSCs have been recognized as a possible source of renewable energy since as early as the 1960s, when photosynthetic microorganisms were used to modify electrodes for improved current production (2). Since then, several adaptations of MSCs have been developed and were recently reviewed (3, 4). The majority of these adaptations utilize photosynthetic processes only at the biofilm anode, such as photosynthetic generation of hydrogen or photosynthetically derived electrons for electricity generation (5–7). Few studies have focused on photosynthetic processes at the biofilm cathode (1, 8–10). For example, He et al. (8), reported on the self-assembly of a synergistic phototrophic-heterotrophic cathode biofilm from a sediment microbial fuel cell (SMFC) (a microbial fuel cell comprised of an organic-matter-oxidizing anode embedded in anoxic marine sediment and an oxygen-reducing cathode positioned in overlying oxic water [11, 12]). In this configuration, current became inhibited due to oxygen intrusion into the sediment. Strik et al. (9) developed a reversible photosynthetic bioelectrode to address the pH gradient limitations encountered in traditional MFCs. This work demonstrated that by first generating an oxygen-producing phototrophic biofilm from wastewater at the cathode of an MFC, all of the reactions could be isolated to a single chamber. This was likely due to the presence of heterotrophic bacteria that were able to drive electrons onto the electrode, as well as reduce O_2.

Previous work by our group indicated that a benchtop sediment/seawater-based MSC configured in an airtight container to exclude ambient oxygen was able to deliver continuous power for >8,000 h with a positive light response without any indication of depletion of power output (1). It was proposed that a phototrophic microbial biofilm on the cathode was responsible for both oxygen generation and the catalysis of oxygen reduction at the cathode required to generate power. In the study reported here, we performed subsequent biocathode enrichments with and without illumination using the progenitor MSC as an inoculum source and defined culturing conditions to separate light-dependent and -independent catalytic components of the MSC biocathode and to identify biofilm community constituents responsible for these catalytic properties. The results indicate that a light-independent consortium of microorganisms is responsible for catalysis of oxygen reduction at the cathode. This consortium appears to carry out respiration of the cathode by coupling electron transfer from the cathode via an insoluble redox cofactor (13) to dissolved atmospheric O_2, where dissolved inorganic carbon is the only available carbon source.

MATERIALS AND METHODS

Microbial fuel cell enrichment experiments. Two sealed sediment-based MSCs were assembled in airtight polypropylene food storage containers

Received 7 February 2013 Accepted 12 April 2013
Published ahead of print 19 April 2013
Address correspondence to Sarah M. Strycharz-Glaven, sarah.glaven@nrl.navy.mil.
Supplemental material for this article may be found at http://dx.doi.org/10.1128/AEM.00431-13.

doi:10.1128/AEM.00431-13

with a circular-plate graphite cathode and anode (6.0 cm by 0.2 cm; total geometric surface area, 0.00520 m^2), similar to those previously described (1). The graphite was pretreated with 0.5 N NaOH, 0.5 N HCl, and deionized water to neutral pH. A titanium bolt used to make an electrical connection to the graphite anode was inserted through a hole in the bottom of the container and sealed with inert epoxy. A titanium wire was inserted through a rubber stopper in the container lid and used to make an electrical connection from the cathode to the graphite anode. A reference electrode (Ag/AgCl, 3 M NaCl; BAS Inc.) was inserted through an airtight rubber stopper in the container lid. Reference electrodes were evaluated for drift in potential both before and after prolonged use in the reactor by testing the open-circuit potential against a new reference electrode dedicated to this purpose. Typically, reference electrodes were offset 2 to 4 mV from the test reference. Approximately 600 ml of seawater-saturated sediment collected from the boat basin of the Rutgers University Marine Field Station near Tuckerton, NJ (1), was added to the container and allowed to settle overnight, covering the anode at a depth of ca. 1 to 2 cm. Approximately 750 ml of sterilized seawater (autoclaved 3 times) collected from the same site was then added to allow as little headspace as possible once the container was sealed. The MSCs were inoculated with fragments of a biofilm harvested from the biocathode of a previously described progenitor MSC (MSC 1 from a previous study) (1), sealed so that the cathode was positioned in seawater above the sediment, and discharged across a resistor (5 kΩ) following equilibration at open circuit for 3 days. The MSCs were maintained in an illuminated incubator for 10 weeks with a 12-h on/off light cycle at 30°C and a total photosynthetic photon flux density (PPFD) of 120 μmol s^{-1} m^{-2}. One of the MSCs, referred to here as the dark MSC, was covered with a blackout cloth to exclude light (PPFD nondetect) in order to inhibit the growth of photosynthetic organisms.

Electrochemical analysis of MSCs. For each MSC, the potentials of the cathode versus the reference electrode (Ag/AgCl) and the cathode versus the anode were monitored either using a multimeter (Keithley 2100) connected to Excel spreadsheet plug-in recording software (Keithley) or using a multichannel potentiostat (Solartron 1470E) under software control (MultiStat; Scribner). Cell voltage was converted to current density by Ohm's law ($V = IR$, where V is voltage, I is current, and R is resistance) and divided by the entire geometric surface area of the anode. Periodically, cyclic voltammetry (CV) was recorded (0.300 V to −0.125 V and back to 0.300 V at a scan rate of 0.0002 V/s) for the cathode, using the anode as the counterelectrode. In this case, current density was determined using the total geometric surface area of the cathode.

Potentiostat enrichment experiments. Scrapings of the cathode biofilm were taken from the dark MSC after 10 weeks once a steady cell voltage was achieved and were subsequently transferred into three potentiostat-poised single-chamber electrochemical reactors, except in the case of abiotic control reactors. Each reactor was a rimmed 100-ml glass beaker with a silicon gasket and Teflon lid held together with stainless steel clamps. The working electrodes were graphite rods (radius, 0.3 cm; height, 6 cm; total geometric surface area, 0.00120 m^2) or graphite flags (1.5 by 1.5 by 0.2 cm; total geometric surface area, 0.00074 m^2) with titanium wire leads (used only for confocal laser scanning microscopy; the current is depicted in Fig. S2 in the supplemental material) inserted into the chamber through rubber stoppers placed in predrilled holes in the Teflon lids. The counterelectrodes were graphite rods (radius, 0.3 cm; height, 6 cm; total geometric surface area, 0.00120 m^2). Single-chamber electrochemical cells were partially assembled and autoclaved. The reference electrodes (Ag/AgCl, 3 M NaCl; BAS Inc.) were sterilized in 10% bleach and added to the sterilized electrochemical reactors. The reactors were filled, minimizing the headspace, with artificial-seawater (ASW) medium for neutrophilic iron-oxidizing bacteria (14), containing 27.50 g NaCl, 3.80 g $MgCl_2 \cdot 6H_2O$, 6.78 g $MgSO_4 \cdot H_2O$, 0.72 g KCl, 0.62 g $NaHCO_3$, 2.79 g $CaCl_2 \cdot 2H_2O$, 1.00 g NH_4Cl, 0.05 g K_2HPO_4, and 1 ml Wolfe's trace mineral solution per liter (14). The medium was brought to a final pH of 6.1 to 6.5 with CO_2. Reactors were maintained in the same illuminated incubator described above at 30°C but were covered in blackout cloth to exclude light (PPFD nondetect). The working electrodes of these reactors were maintained at 0.100 V (approximately 0.310 V versus a standard hydrogen electrode [SHE]) so as to act as cathodes using a multichannel potentiostat (Solartron 1470E) under software control (MultiStat; Scribner). The background current during chronoamperometry and the CV (0.300 V to −0.125 V and back to 0.300 V at a scan rate of 0.0002 V/s) were recorded for each reactor before inoculation, and subsequently, the CV of biocathodes was recorded using the same parameters.

Clone library generation and phylogenetic analysis. Biofilms were sampled for metagenomic DNA isolation and analysis once a stable cell voltage was maintained for 10 weeks (sediment/seawater-based MSCs) or stable current (applied potential reactors) was achieved by scraping the biofilm from the electrode with a clean, ethanol flame-sterilized razor blade. Biofilm samples were resuspended in isotonic wash buffer, homogenized by brief vortexing, and pelleted at 10,000 × *g* for 2 min. The supernatant was removed and discarded, and the pellets were stored at −20°C. Total metagenomic DNA was extracted from the electrode scrapings using a soil DNA extraction kit according to the manufacturer's instructions (UltraClean soil DNA isolation kit; Mo Bio). Between 0.5 and 1 ng/μl of metagenomic DNA was used to amplify the entire 16S rRNA gene using 16S rRNA universal primers (forward primer 49F, 5′-TNANACATGCAAGTCGRRCG-3′; reverse primer 1510R, 5′-RGYTACCTTGTTACGACTT-3′ [15]) and the following thermocycling conditions: 94°C for 3 min; 34 cycles of 94°C (30 s), 50°C (30 s), and 72°C (1 min); and 72°C for 10 min. The amplification products were purified using the MinElute PCR purification kit (Qiagen). DNA clone libraries were constructed from purified PCR fragments using a Topo TA cloning kit (Invitrogen) according to the manufacturer's instructions. Positive colonies were selected and placed into a 96-well plate for PCR amplification of the cloned insert for sequencing using M13 forward (5′-GTAAAACGACGGCCAGT-3′) and reverse (5′-CAGGAAACAGCTATGAC-3′) primers. The amplification products were purified using the ExoSap-It for PCR Product Clean-Up (Affymetrix), and sequencing was performed using the M13F primer on an ABI 3730 XL (Applied Biosystems). The resulting sequences were searched using the National Center for Biotechnology Information database (http://www.ncbi.nlm.nih.gov/BLAST/) and deposited in GenBank. 16S rRNA gene sequences were randomly selected from each sample and used to generate phylogenetic trees based on the neighbor-joining method (16) using the MEGA4 program (17).

Scanning electron microscopy. The bottom 1 cm of one of the working electrodes of the aforementioned three-electrode reactors was removed once a stable current was achieved by first scoring the electrode with an ethanol flame-sterilized razor blade and breaking off the scored portion using needle nose pliers. The electrode was rinsed in sterile, filtered (0.2 μm) isotonic wash buffer consisting of 4.19 g MOPS (morpholinepropanesulfonic acid), 0.60 g $NaH_2PO_4 \cdot H_2O$, 0.10 g KCl, 5.00 g NaCl, and 10 ml Mg-Ca mixture (3.00 g/liter $MgSO_4 \cdot 7H_2O$, 0.10 g/liter $CaCl_2 \cdot 2H_2O$) per liter. The sample was fixed for 2 h in filter-sterilized 2% glutaraldehyde–phosphate-buffered saline (PBS) solution (pH 8.0), rinsed with PBS, and dehydrated using a graded acetone series (35, 50, 70, 90, 100, 100, 100, 100, 100, and 100% for 10 min each), followed by 50% hexamethyldisilazane (HMDS) in acetone for 10 min, 100% HMDS twice for 10 min each time, and air drying. Following dehydration, the sample was sputter coated (Cressington sputter coater 108auto) and analyzed using a scanning electron microscope (Carl Zeiss SMT Supra 55) at 4 kV.

Confocal laser scanning microscopy. Graphite flag electrodes were removed from the electrochemical reactors once maximum current was achieved (see Fig. S2 in the supplemental material) and rinsed twice in 1× PBS, pH 7.4 (Excelleron). Biofilms were stained according to the manufacturer's instructions with the LIVE/DEAD BacLight Bacterial Viability Kit (Invitrogen). Staining of all electrodes was carried out in 1× PBS, pH 7.4, for 10 min at room temperature in the dark. The electrodes were rinsed once with 1× PBS, pH 7.4; allowed to destain in 1× PBS, pH 7.4, for 10 min; and mounted in a single-well chambered cover glass slide

(Lab-Tek) with several microliters of mounting oil (Prolong Gold Antifade; Invitrogen). Imaging was carried out using a Nikon TE-2000e inverted confocal microscope (Nikon) with a Nikon CFI Apo TIRF 100× (numerical aperture, 1.49) oil objective. Two wavelengths, 488 nm and 514 nm, were used to excite the fluorescent stains. A minimum of 8 fields were imaged and processed with the ImageJ software program (http://imagej.nih.gov/ij/). Three random image stacks were used to determine the mean biofilm height by measuring the height at 18 random points for each stack using ImageJ.

Nucleotide sequence accession numbers. The sequences developed in the study were deposited in GenBank under accession numbers KC569994 to KC570221.

RESULTS

Electrochemical characterization and microbial-community analysis of the MSC biocathode. Previously, Malik et al. (1) reported on the development of a spontaneously formed biocathode biofilm using a sealed sediment/seawater-based MSC. In the previous study, the MSC demonstrated a positive current response when the cathode was illuminated, and visual inspection of the biofilm revealed a thick, greenish mat suggestive of a phototrophic biofilm (18). A fragment of the biocathode biofilm from this progenitor MSC was used as an inoculum source for the sediment/seawater-based MSCs reported here, developed under defined temperature and light conditions. Biocathodes were incubated under either illuminated or dark conditions to determine if formation of a catalytically active biofilm was dependent upon light. A diurnal light-dependent current was established by the illuminated MSC within 2 days following discharge across the resistor (5 kΩ) (see Fig. S3A in the supplemental material). This result is consistent with that of the progenitor cell (1), indicating formation of a comparable biocathode. In contrast, it took 2 weeks for the dark MSC to establish a stable current when initially discharged (see Fig. S3B in the supplemental material). Current from the dark MSC did not follow a diurnal pattern and was 2-fold greater in magnitude than that from the illuminated MSC. The higher current of the dark reactor than the illuminated reactor indicated a potentially negative effect of prolonged illumination despite the fact that the illuminated reactor formed an electrochemically active biofilm more quickly.

To further explore the electrochemical characteristics of the illuminated and dark MSC biocathodes, cyclic voltammetry was used to qualitatively assess their catalytic properties once a stable current was achieved. Slow-scan CV (0.0002 V/s) of the biocathodes from the illuminated (day 3) and dark (day 23) MSCs displayed Nernstian (i.e., sigmoid-shaped) catalytic current versus potential dependencies, with nearly identical midpoint potentials (the potential at which the current is half of the maximum catalytic current observed at more negative potentials) of ca. 0.196 V ± 0.010 V versus Ag/AgCl (Fig. 1). This result suggests the illuminated and dark biocathodes utilize an immobilized redox cofactor to mediate heterogeneous electron transfer between the cathode and the biofilm and that the rate of heterogeneous electron transfer is higher than those of other biofilm electron transport processes (13). The fact that the midpoint potential and shape of the catalytic wave were nearly identical for both the dark and illuminated biocathodes suggests that both utilize the same heterogeneous redox cofactor or different cofactors with similar redox potentials. The biocathode catalytic current was passivated in the illuminated MSC after a period of 8 weeks (see Fig. S4A in the supplemental material), which could account for the lower current of this reactor than of the dark MSC. Possible explanations for biocathode passivation in the illuminated reactor are toxicity to the catalytic component of the biofilm from photosynthetic activity, as discussed below, or limitation of diffusion of the substrate through the biofilm following proliferation of noncatalytic photosynthetic organisms. Catalytic current was detected at the cathode of the dark MSC during the same time (see Fig. S4B in the supplemental material).

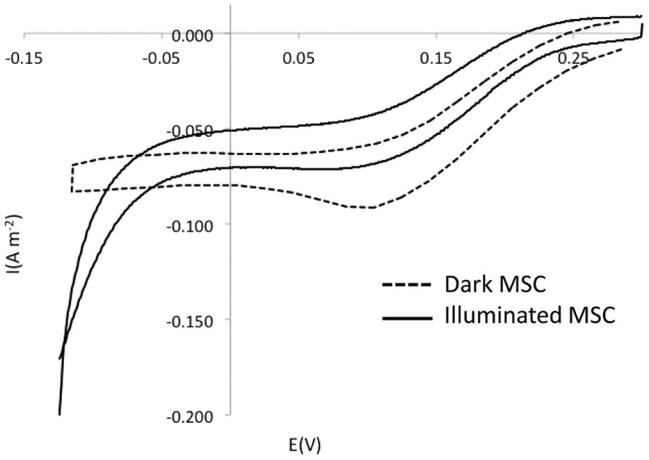

FIG 1 Slow-scan CV (0.0002 V/s) of the dark sediment/seawater-based MSC at day 23 and the illuminated sediment/seawater-based MSC at day 3 following discharge across a 5-kΩ resistor.

16S rRNA gene clone libraries generated from biofilm scrapings from the cathode of the dark MSC collected at the stable cell current revealed a bacterial consortium whose predominant constituents belong to *Gammaproteobacteria*, *Alphaproteobacteria*, and *Betaproteobacteria* (88.2% of the clones; see Fig. S5A in the supplemental material). The closest matches to known, identified 16S rRNA genes included a number of sulfur-oxidizing marine bacteria and marine symbionts (≥90% sequence identity), a neutrophilic iron-oxidizing *Sideroxydans* sp. (≥90% sequence identity) (19), and other marine bacteria (<90% sequence identity) (Fig. 2A). Identical analysis of biofilm scrapings from the cathode of the illuminated MSC at stable cell current revealed a community dominated by *Cyanobacteria* (69.0%), with *Proteobacteria* (13.1%) representing a smaller fraction than in the dark MSC (see Fig. S5B in the supplemental material). The closest matches to known, identified 16S rRNA genes from the illuminated biocathode biofilm included *Cyanobacteria* (100%), *Bacteroidetes* (100% sequence identity), *Acidobacteria* (100% sequence identity), various *Alphaproteobacteria* (95 to 100% sequence identity), and *Planctomycetes* (66 to 93% sequence identity) (Fig. 2B).

Enrichment of the MSC biocathode in a three-electrode system. Further enrichment of the dark sediment/seawater-based MSC biocathode biofilm was carried out in order to characterize catalytic activity independently of illumination and under more rigorously defined culturing conditions. Scrapings from the biocathode of the dark sediment/seawater-based MSC served as the inoculum for three-electrode-configured electrochemical reactors maintained in the dark and containing sterile, aerobic ASW medium at nearly neutral pH, previously developed for iron-oxidizing bacteria (14). These reactor conditions were chosen based

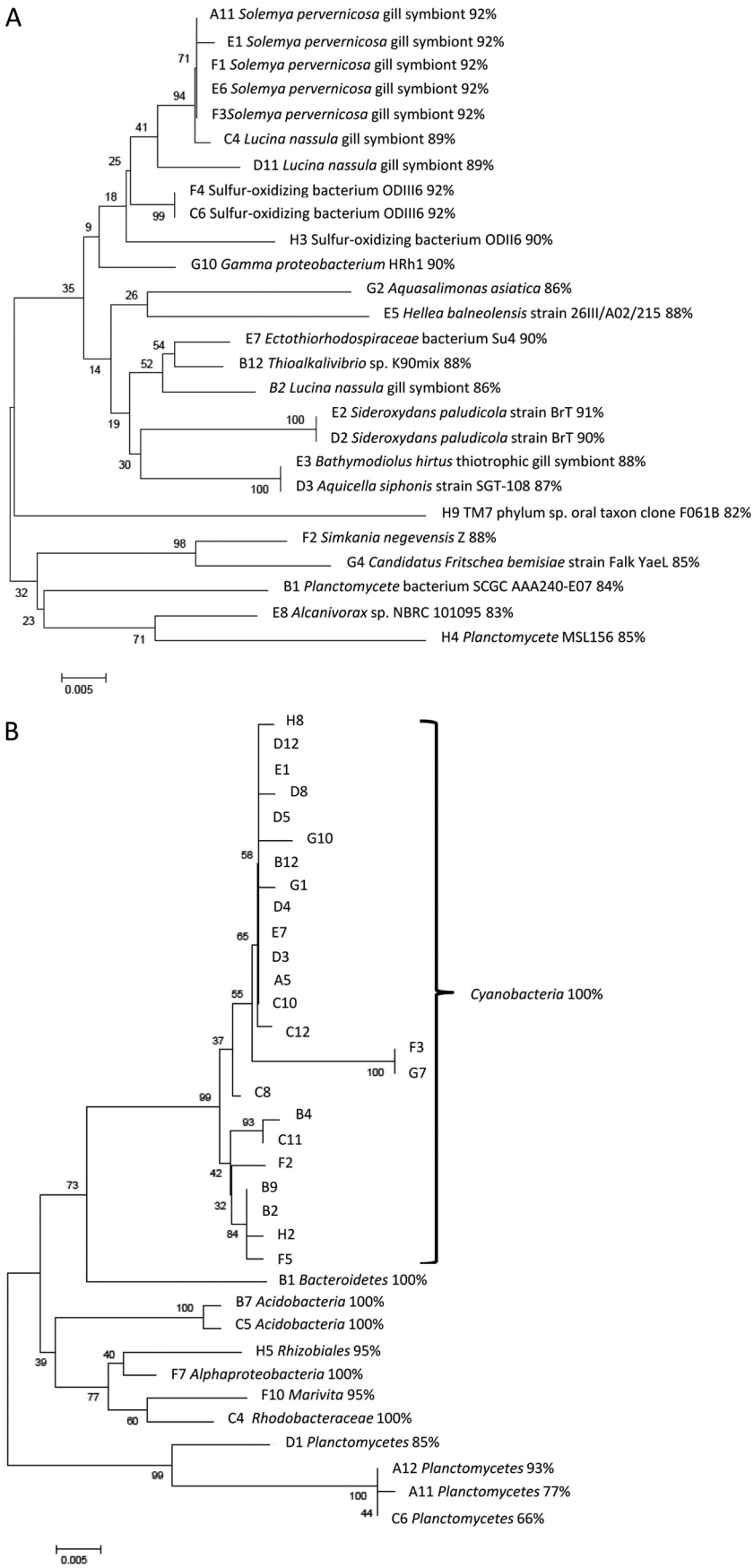

FIG 2 16S rRNA gene clone libraries were generated from DNA extracted from the dark (A) and illuminated (B) sediment/seawater-based MSC biocathodes. Representative sequences were selected at random and aligned, and phylogenetic trees were generated using Mega4 software. Bootstrap values are listed at each branch point. Percentages are sequence identities to the closest matches to 16S rRNA genes of known organisms. The scale bar indicates estimated sequence divergence.

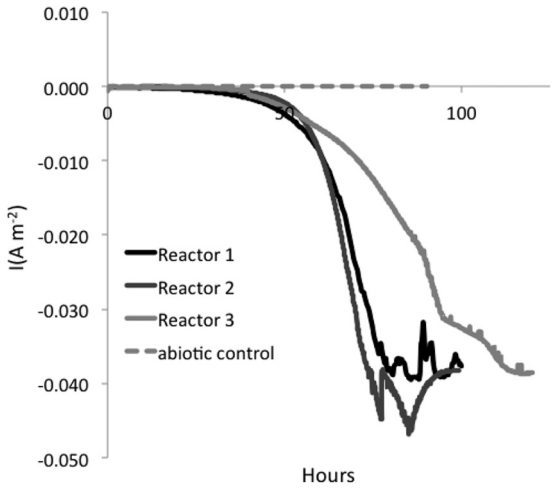

FIG 3 Chronoamperometry of dark-MSC biocathode enrichment reactors. The working electrode was set at 0.100 V versus Ag/AgCl to achieve the maximum current density recorded in the original illuminated and dark sediment/seawater-based MSCs. Within 48 h after inoculation, an increase in current (plotted here as negative current to indicate a cathode reaction) was observed above the abiotic control.

on identification of an iron-oxidizing bacterium from 16S rRNA gene profiling of the dark MSC biocathode and the likelihood that iron-oxidizing bacteria would be candidates for microbial-cathode catalysis. The working electrodes of these reactors were set at 0.100 V (versus Ag/AgCl) to act as cathodes based on midpoint potentials observed for the MSC biocathodes in Fig. 1. A control reactor was included under identical conditions but without electrode scrapings. Current increased in magnitude in the inoculated reactors, but not in the control reactor, within 48 h of inoculation and achieved a maximum current density of between −0.035 A m^{-2} and −0.045 A m^{-2} within 3 days (Fig. 3).

Slow-scan (0.0002 V/s) CV recorded at maximum current resulted in a sigmoid-shaped curve with midpoint potential at approximately 0.205 V versus Ag/AgCl, suggesting utilization of a heterogeneous electron transfer cofactor by the biofilm of the enriched biocathode that was the same or similar to that observed in both the dark and illuminated sediment/seawater-based MSCs (Fig. 4). A qualitative comparison (Fig. 4, open circles) was made to a catalytic CV expected when heterogeneous electron transfer between the cathode and biofilm is mediated by a redox cofactor whose oxidation state is governed by the electrode potential, in accordance with the Nernst equation (equation 16 in the work of Strycharz-Glaven et al. [20]). This comparison was in agreement with observations made for the CV of the dark and illuminated MSCs, where the rate of heterogeneous electron transfer is higher than those of other biofilm electron transport processes, analogous to a model proposed for *Geobacter* bioanodes (13). The CV of the control reactor was featureless (Fig. 4). When the reactor was purged with N_2, the catalytic current was no longer observed, indicating that O_2 is the terminal electron acceptor (21). A small set of voltammetric peaks was observed in the CV of N_2-purged reactors near the midpoint potential of the catalytic curve, which we attribute to the heterogeneous electron transfer cofactor (Fig. 4, inset) (13). Replacing the medium with fresh, oxygenated artificial seawater restored the catalytic current (Fig. 4).

16S rRNA gene clone library analysis of the enriched dark bio-

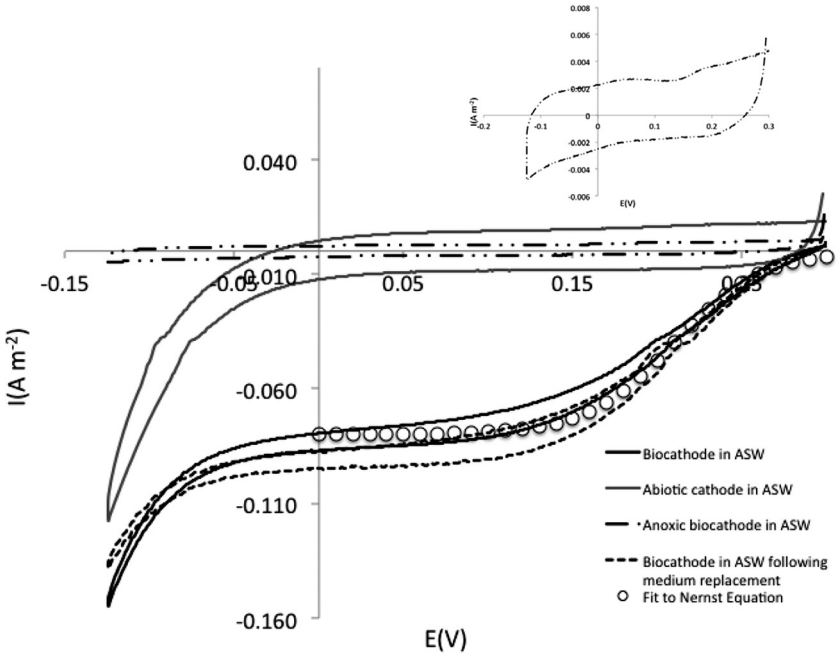

FIG 4 Slow-scan CV (0.0002 V/s) of the enriched dark biocathode revealed catalytic features similar to those observed in the dark and illuminated sediment/seawater-based MSCs (solid black line). Catalytic current was not observed in control reactors (solid gray line). Single-chamber reactors were purged with nitrogen gas until catalytic current was no longer detected, and the nonturnover CV was recorded (dashed-dotted lines and inset). When the medium was replaced with fresh artificial-seawater medium, catalytic current was restored (dashed line). Slow-scan voltammetry was fitted to a first approximation with the Nernst equation according to equation 16 in reference 20 (open circles).

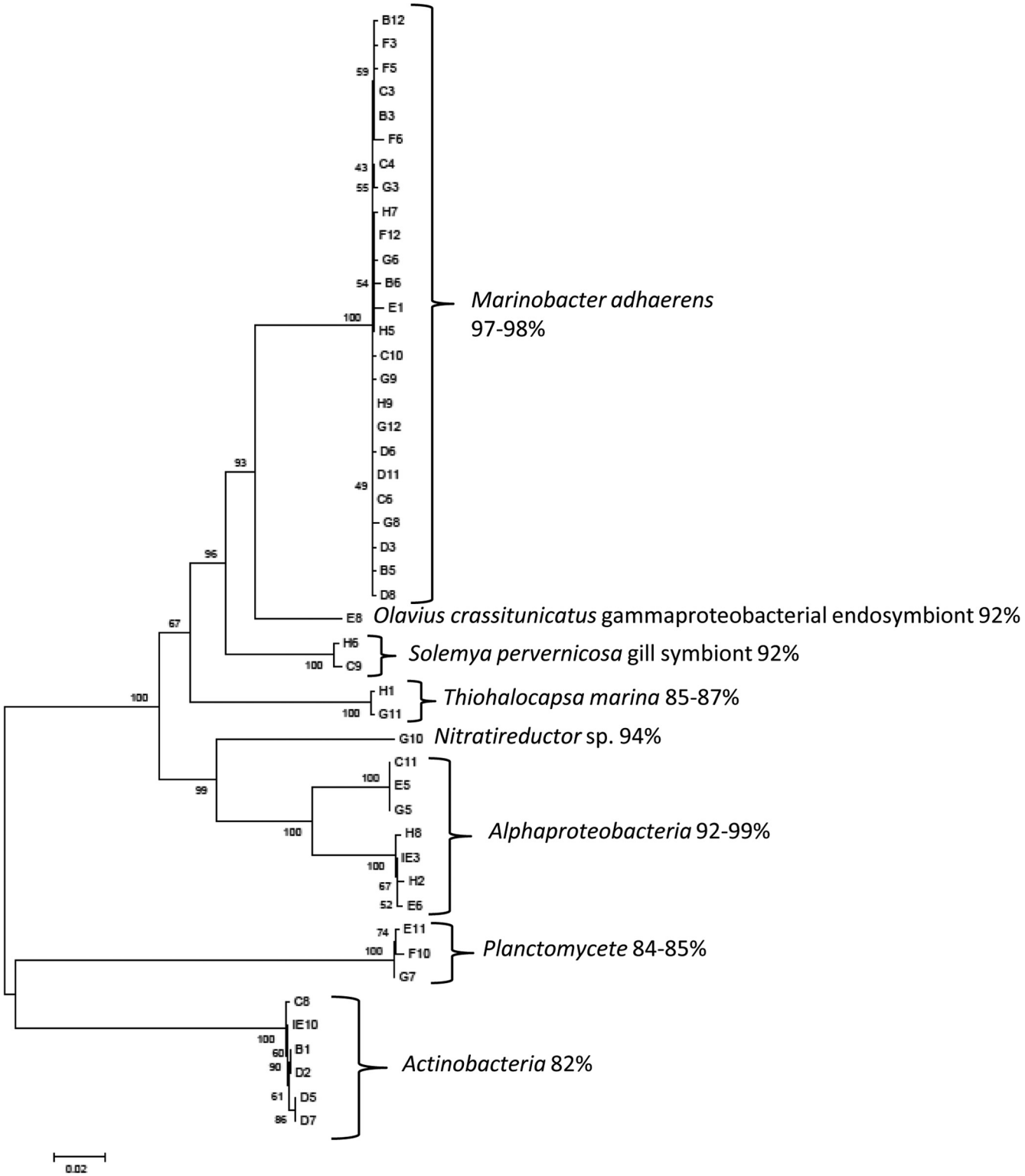

FIG 5 16S rRNA gene clone libraries were generated from electrode-extracted DNA from the enriched biocathode, representative sequences were aligned, and phylogenetic trees were generated using Mega4 software. Bootstrap values are listed at each branch point. Percentages are sequence identities to the closest matches to 16S rRNA genes of known organisms. The scale bar indicates estimated sequence divergence.

cathode showed the majority of clones were identified as *Proteobacteria* (Fig. 5). Over half of the sequences most closely matched *Marinobacter adhaerens* (97 to 98% identity). Additional matches within the *Gammaproteobacteria* included sulfur-oxidizing symbionts of marine mammals (92% identity) and phototrophic purple sulfur bacteria (87% identity). Other sequences matched *Alphaproteobacteria* (92 to 99% identity), including one match to a *Nitratireductor* sp. (94% identity). A number of sequences re-

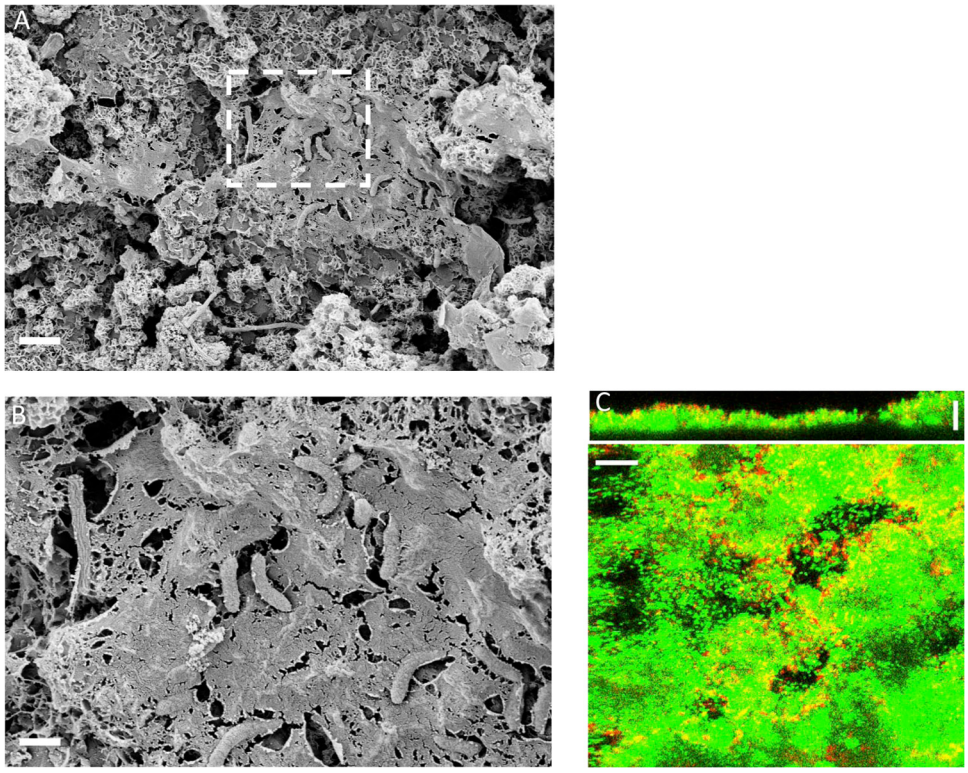

FIG 6 (A) Scanning electron microscopy was performed to visualize the surface of the enriched biocathode. The dashed line represents the area of the electrode enlarged in panel B. (B) In areas where the biofilm appeared to coat the electrode surface, cells were associated with extracellular biofilm material. (C) Confocal laser scanning microscopy was performed on a separate graphite flag electrode to determine the average biofilm thickness and viability. The average height at the location represented by the image shown is 5.244 ± 2.141 μm ($n = 9$). Biofilm thickness varied over the surface of the electrode and ranged from ca. 2.3 to 8.2 μm. Scale bars, 2 μm (A and B) and 10 μm (C).

turned weak matches to *Actinobacteria* and *Planctomycetes* (82 to 85% identity).

Scanning electron microscopy of the biocathode biofilm demonstrated at least two morphologically distinct rod-shaped cell types among what appeared to be dehydrated extracellular matrix material (Fig. 6A and B). Confocal laser scanning microscopy following a viability stain (LIVE/DEAD) revealed that the majority of cells had intact membranes (green-stained cells). A representative image captured by scanning through the z axis of the biofilm is shown in Fig. 6C. Cell coverage was continuous over the majority of the surface of the electrode, with the biofilm projecting up to 8.2 μm into the surrounding medium, indicating that the biofilm was multiple cell layers thick.

DISCUSSION

We previously reported on the development of a sediment/seawater-based MSC hypothesized to be continuously driven by photosynthetic processes occurring at the biocathode (1). In the current study, we sought to begin to understand the microbial and catalytic underpinnings of such MSCs by determining the contribution of photosynthetic biocathode reactions versus nonphotosynthetic biocathode reactions to current through electrochemical characterization. In addition, we sought to identify catalytic biocathode biofilm constituents following enrichment in single-chamber electrochemical reactors operated with an applied potential to maximize the biocathode current.

Perhaps the most interesting finding was that the catalytic activity at the biocathode of the sediment/seawater-based MSC was independent of light and that, under the conditions tested here, illumination had an inhibitory effect on biocatalysis at the electrode. Current density in both the illuminated and dark MSCs reported here was comparable to that reported for the progenitor cell (ca. 0.005 to 0.040 A m^{-2}) (1). The dark MSC, however, achieved a maximum current density that was twice that of the illuminated MSC, which we attribute to passivation of catalytic activity at the biocathode. Slow-scan CV of both the illuminated and dark MSC biocathodes indicated Nernstian current-potential dependencies with nearly identical midpoint potentials, suggesting utilization of similar, if not the same, heterogeneous electron transfer cofactors.

Passivation of the catalytic activity of the illuminated biocathode occurred over time and may be correlated with the proliferation of photosynthetic microorganisms, which made up nearly 70% of all sequences retrieved from 16S rRNA gene profiling of the illuminated biofilm. Cyanobacterial-bacterial-mat consortia are highly stratified biofilms containing photosynthetic, heterotrophic, and chemoautotrophic microorganisms living in suboxic and anoxic zones dependent upon complex chemical gradients that naturally form within the biofilm (22, 23). If O_2 consumption occurs at a lower rate than photosynthetic O_2 generation and diffusion, suboxic and anoxic metabolism can be disrupted (22, 24). Such a phenomenon may have occurred in the case of the illuminated MSC if bacteria receiving electrons from the electrode prefer suboxic conditions and O_2 reduction is not sustained at a rate high

enough to keep O_2 concentrations at a metabolically acceptable level. This would likely be the case if the electrode catalytic member of the consortium is a neutrophilic iron oxidizer thriving at the oxic-anoxic interface (25–27), such as *Sideroxydans* sp. or *Marinobacter* sp., both of which were detected in dark-biocathode 16S rRNA gene profiles. Although passivation was not observed in the progenitor cell (1), differences in light intensity (natural versus controlled) and temperature (ambient versus controlled) may have contributed to differences in O_2 cycling. Potential toxicity due to photosynthetically derived O_2 has implications for future designs of MSC reactors, where illumination may ultimately negate the benefits of a self-sustaining system. As such, further investigations of the MSC conditions are necessary to fully exploit the photosynthetic reactions. The possibility that proliferation of photosynthetic organisms prevents substrate diffusion in and out of the catalytic portion of the biofilm, and thus limits current, also needs to be explored.

Enrichment of the biocathode from the dark sediment/seawater-based MSC resulted in a robust, aerobic biofilm catalyzing O_2 reduction and was developed with no carbon source other than dissolved inorganic carbon. A qualitative comparison of experimental slow-scan CV (0.0002 V/s) to a calculated catalytic CV based on the Nernst equation indicated that heterogeneous electron transfer between the cathode and biofilm is mediated by a redox cofactor whose oxidation state is governed by the electrode potential and is consistent with catalytic current that is not limited by the rate of this reaction or by the rate of cellular turnover of oxygen. Rather, electron transfer appears to be limited by either the rate of transport of electrons through the biofilm, delivery of electrons into cells comprising the biofilm beyond the electrode interface (assuming electron transfer at a distance from the electrode analogous to that of anode biofilms of *Geobacter sulfurreducens* [13]), or diffusion of the electron acceptor (O_2) into the biofilm. In the last case, a deviation from the classic Nernstian catalytic CV would be expected to occur (13); however (see Fig. 3H and I in reference 13), it might not be detectable here. When the medium was replaced in the batch reactor, no loss of current was observed, also indicating that electron transfer reactions are likely mediated by an insoluble redox cofactor. Although it is unclear at this time whether cells at a distance from the electrode surface participate in electron exchange, microscopy reveals a multiple-cell-layer-thick biofilm at the biocathode. Viability staining identifies the majority of these cells as "live," suggesting that they may be prospering from electrode reactions.

At higher scan rates, voltammetric peaks could not be resolved (not shown), suggesting that the rate of the heterogeneous electron transfer reaction and/or electron transport and mass transport through the biofilm is relatively low compared to that observed for *G. sulfurreducens* biofilms grown on anodes (13, 28). The small size of peaks observed during nonturnover CV suggests that the total abundance of the electron transfer cofactor was also considerably smaller than that of *G. sulfurreducens* biofilms grown on anodes, consistent with the lower catalytic current observed here (13, 20, 29).

Introduction of photosynthetically derived oxygen to the cathode compartments of MFCs to regenerate the oxidant has previously been proposed using algal cultures (3, 4, 30). However, to our knowledge, only a few studies have reported on the electrochemical activity of a phototrophic biocathode (1, 8, 9) where photosynthetic reactions are confined to the electrode biofilm, and the CV was not reported in these studies. CV has been used to analyze O_2 reduction at nonphotosynthetic biocathodes enriched from various inocula (21, 31, 32). Ter Heijne et al. (21) reported a CV shaped similarly to that observed in this study when a wastewater biocathode was developed at 0.150 V versus Ag/AgCl on graphite in a flowthrough reactor with a reported maximum limiting current of 295 mA m^{-2}. In this case, the authors determined that mass transport of O_2 to the electrode surface, as well as within the biofilm, is a limiting factor and suggested photosynthesis as a means to deliver O_2 to the biofilm. Mass transport of O_2 is predicted to be one limiting factor in our current system; however, as noted above, high concentrations of O_2 within the biofilm may also lead to passivation. The reintroduction of photosynthetic organisms to provide O_2 directly at the biocathode-electrode interface may improve this limitation only if optimal biofilm O_2 gradients can be established.

The community composition of electrocatalytic photosynthetic biocathodes has not been explored in depth. In one study, He et al. (8) found that the biocathode consortium of a photosynthetic open-air MSC was comprised of *Cyanobacteria* and *Proteobacteria*, among others, which is consistent with our illuminated-MSC observations. Although no exact matches to sequences identified from the illuminated MSC were observed in the dark MSC, *Proteobacteria* were prevalent on both biocathodes. Reports on spontaneously formed, nonphotosynthetic marine biocathodes (33, 34) have identified a number of potential microbial catalysts as part of biofilm consortia (28, 30, 35). The major finding from these studies appears to be that biocathode biofilms enriched from the marine environment perform optimally as a consortium rather than in pure culture and that *Proteobacteria* are typically observed.

Phylogenetic analysis of the enriched biocathode consortium in the three-electrode reactor indicated the predominance of *Gammaproteobacteria*, specifically *Marinobacter*. Although *Marinobacter* spp. were not detected in the initial 16S rRNA gene profiling of the dark MSC, their abundance may have been too low compared to other organisms in the sample. To our knowledge, the presence of *Marinobacter* has been noted only once before as part of a biocathode biofilm consortium, and when tested in pure culture, it did not catalyze cathodic reactions (34). *Marinobacter* spp. are ubiquitous, biofilm-forming marine bacteria known to oxidize iron under aerobic, circumneutral conditions (36) and have been found to be associated with photosynthetic marine organisms (37). The facultative mixotroph *Marinobacter aquaeolei* VT8 is the best characterized of the *Marinobacter* spp. and has 47 genes encoding cytochrome proteins potentially participating in iron oxidation (in comparison, *Shewanella oneidensis* MR-1 has 66) (36). The abundance of potential cytochrome proteins is significant, because *c*-type cytochromes of *G. sulfurreducens* are known to be essential for anode biofilm electron transfer (38). Complementary metagenomic analysis of the biocathode enrichment is under way to further explore the diversity and structure of the community.

Conclusions. Optimization of the MSC has the potential to provide continuous renewable power when the products of the anodic reactions provide the reactants at the cathode, and vice versa, with only sunlight required to generate power. In this study, we have presented a further characterization of the electrochemical properties of both the photosynthetic and nonphotosynthetic

constituents of an MSC biocathode. We have found that the same voltammetric catalytic feature is observed at the electrode-biofilm interface in the presence or absence of light. Prolonged illumination had a deleterious effect on biocathode catalytic activity, possibly due to toxicity of photosynthetic by-products or substrate diffusion limitations caused by proliferation of photosynthetic organisms. Future studies will be aimed at reintroducing the photosynthetic component of the biocathode without passivating the catalytic component.

Enrichment of the dark-MSC biocathode using a three-electrode configuration led to development of a multispecies biofilm at the biocathode that was dominated by *Gammaproteobacteria*, specifically *Marinobacter*. Enriched biocathode biofilms did not require any additional carbon source other than dissolved inorganic carbon for growth and showed features during CV similar to those of both the illuminated and dark sediment/seawater-based MSC biocathodes. Qualitative analysis of CV from the enriched biocathodes showed that current may be limited by electron transfer between redox cofactors within the biofilm, electron transfer into cells located beyond the electrode surface, or mass transfer of O_2 to the biocathode. The enriched biocathode biofilm discussed here will be further developed for bioelectrochemical system applications where robust marine microbial biocatalysts that can grow directly by incorporating inorganic carbon are desired, such as for cathodic O_2 reduction in MFCs and for microbial electrosynthesis (39).

ACKNOWLEDGMENTS

This work was supported by the Office of Naval Research via U.S. Naval Research Laboratory core funds.

The opinions and assertions contained herein are those of the authors and are not to be construed as those of the U.S. Navy, the military services at large, or the U.S. Government.

REFERENCES

1. **Malik S, Drott E, Grisdela P, Lee J, Lee C, Lowy DA, Gray S, Tender LM.** 2009. A self-assembling self-repairing microbial photoelectrochemical solar cell. Energy Environ. Sci. **2**:292–298.
2. **Berk RS, Canfield JH.** 1964. Bioelectrochemical energy conversion. Appl. Microbiol. **12**:10–12.
3. **Strik DPBTB, Timmers RA, Helder M, Steinbusch KJJ, Hamelers HVM, Buisman CJN.** 2011. Microbial solar cells: applying photosynthetic and electrochemically active organisms. Trends Biotechnol. **29**:41–49.
4. **Rosenbaum M, He Z, Angenent LT.** 2010. Light energy to bioelectricity: photosynthetic microbial fuel cells. Curr. Opin. Biotechnol. **21**:259–264.
5. **Rosenbaum M, Schroder U, Scholz F.** 2005. Utilizing the green alga *Chlamydomonas reinhardtii* for microbial electricity generation: a living solar cell. Appl. Microbiol. Biotechnol. **68**:753–756.
6. **Zou YJ, Pisciotta J, Billmyre RB, Baskakov IV.** 2009. Photosynthetic microbial fuel cells with positive light response. Biotechnol. Bioeng. **104**: 939–946.
7. **Pisciotta JM, Zou Y, Baskakov IV.** 2010. Light-dependent electrogenic activity of cyanobacteria. PLoS One **5**(5):e10821. doi:10.1371/journal.pone.0010821.
8. **He Z, Kan J, Mansfeld F, Angenent LT, Nealson KH.** 2009. Self-sustained phototrophic microbial fuel cells based on the synergistic cooperation between photosynthetic microorganisms and heterotrophic bacteria. Environ. Sci. Technol. **43**:1648–1654.
9. **Strik DP, Hamelers HV, Buisman CJ.** 2010. Solar energy powered microbial fuel cell with a reversible bioelectrode. Environ. Sci. Technol. **44**: 532–537.
10. **Cao XX, Huang X, Liang P, Boon N, Fan MZ, Zhang L, Zhang XY.** 2009. A completely anoxic microbial fuel cell using a photo-biocathode for cathodic carbon dioxide reduction. Energy Environ. Sci. **2**:498–501.
11. **Reimers C, Tender L, Fertig S, Wang W.** 2001. Harvesting energy from the marine sediment-water interface. Environ. Sci. Technol. **35**:192–195.
12. **Tender L, Reimers C, Stecher H, Holmes D, Bond D, Lowy D, Pilobello K, Fertig S, Lovley D.** 2002. Harnessing microbially generated power on the seafloor. Nat. Biotechnol. **20**:821–825.
13. **Strycharz SM, Malanoski AP, Snider RM, Yi H, Lovley DR, Tender LM.** 2011. Application of cyclic voltammetry to investigate enhanced catalytic current generation by biofilm-modified anodes of *Geobacter sulfurreducens* strain DL1 vs. variant strain KN400. Energy Environ. Sci. **4**:896–913.
14. **Emerson D, Floyd MM.** 2005. Enrichment and isolation of iron-oxidizing bacteria at neutral pH. Environ. Microbiol. **397**:112–123.
15. **Moyer CL, Dobbs FC, Karl DM.** 1994. Estimation of diversity and community structure through restriction-fragment-length-polymorphism distribution analysis of bacterial 16S ribosomal-RNA genes from a microbial mat at an active, hydrothermal vent system, Loihi Seamount, Hawaii. Appl. Environ. Microbiol. **60**:871–879.
16. **Saitou N, Nei M.** 1987. The neighbor-joining method: a new method for reconstructing phylogenetic trees. Mol. Biol. Evol. **4**:406–425.
17. **Tamura K, Dudley J, Nei M, Kumar S.** 2007. MEGA4: Molecular Evolutionary Genetics Analysis (MEGA) software version 4.0. Mol. Biol. Evol. **24**:1596–1599.
18. **Roeselers G, Loosdrecht M, Muyzer G.** 2008. Phototrophic biofilms and their potential applications. J. Appl. Phycol. **20**:227–235.
19. **Weiss JV, Rentz JA, Plaia T, Neubauer SC, Merrill-Floyd M, Lilburn T, Bradburne C, Megonigal JP, Emerson D.** 2007. Characterization of neutrophilic Fe(II)-oxidizing bacteria isolated from the rhizosphere of wetland plants and description of *Ferritrophicum radicicola* gen. nov. sp. nov., and *Sideroxydans paludicola* sp. nov. Geomicrobiol. J. **24**:559–570.
20. **Strycharz-Glaven SM, Tender LM.** 2012. Study of the mechanism of catalytic activity of *G. sulfurreducens* biofilm anodes during biofilm growth. ChemSusChem **5**:1106–1118.
21. **Ter Heijne A, Strik DP, Hamelers HV, Buisman CJ.** 2010. Cathode potential and mass transfer determine performance of oxygen reducing biocathodes in microbial fuel cells. Environ. Sci. Technol. **44**:7151–7156.
22. **Paerl HW, Pinckney JL, Steppe TF.** 2000. Cyanobacterial-bacterial mat consortia: examining the functional unit of microbial survival and growth in extreme environments. Environ. Microbiol. **2**:11–26.
23. **Ramsing NB, Kuhl M, Jorgensen BB.** 1993. Distribution of sulfate-reducing bacteria, O_2, and H_2S in photosynthetic biofilms determined by oligonucleotide probes and microelectrodes. Appl. Environ. Microbiol. **59**:3840–3849.
24. **Stewart PS, Franklin MJ.** 2008. Physiological heterogeneity in biofilms. Nat. Rev. Microbiol. **6**:199–210.
25. **Hedrich S, Schlomann M, Johnson DB.** 2011. The iron-oxidizing proteobacteria. Microbiology **157**:1551–1564.
26. **Weber KA, Achenbach LA, Coates JD.** 2006. Microorganisms pumping iron: anaerobic microbial iron oxidation and reduction. Nat. Rev. Microbiol. **4**:752–764.
27. **Emerson D, Fleming EJ, McBeth JM.** 2010. Iron-oxidizing bacteria: an environmental and genomic perspective. Annu. Rev. Microbiol. **64**:561–583.
28. **Erable B, Feron D, Bergel A.** 2012. Microbial catalysis of the oxygen reduction reaction for microbial fuel cells: a review. ChemSusChem **5**:975–987.
29. **Strycharz-Glaven SM, Snider RM, Guiseppi-Elie A, Tender LM.** 2011. On the electrical conductivity of microbial nanowires and biofilms. Energy Environ. Sci. **4**:4366–4379.
30. **Rosenbaum M, Schroder U.** 2010. Photomicrobial solar and fuel cells. Electroanalysis **22**:844–855.
31. **Freguia S, Tsujimura S, Kano K.** 2010. Electron transfer pathways in microbial oxygen biocathodes. Electrochim. Acta **55**:813–818.
32. **Rabaey K, Read ST, Clauwaert P, Freguia S, Bond PL, Blackall LL, Keller J.** 2008. Cathodic oxygen reduction catalyzed by bacteria in microbial fuel cells. ISME J. **2**:519–527.
33. **Parot S, Vandecandelaere I, Cournet A, Delia ML, Vandamme P, Berge M, Rogues C, Bergel A.** 2011. Catalysis of the electrochemical reduction of oxygen by bacteria isolated from electro-active biofilms formed in seawater. Bioresour. Technol. **102**:304–311.
34. **Erable B, Vandecandelaere I, Faimali M, Delia ML, Etcheverry L, Vandamme P, Bergel A.** 2010. Marine aerobic biofilm as biocathode catalyst. Bioelectrochemistry **78**:51–56.
35. **Huang LP, Regan JM, Quan X.** 2011. Electron transfer mechanisms, new applications, and performance of biocathode microbial fuel cells. Bioresour. Technol. **102**:316–323.
36. **Singer E, Webb EA, Nelson WC, Heidelberg JF, Ivanova N, Pati A,**

Edwards KJ. 2011. Genomic potential of *Marinobacter aquaeolei*, a biogeochemical "opportunitroph".Appl. Environ. Microbiol. **77**: 2763–2771.
37. **Amin SA, Green DH, Hart MC, Kupper FC, Sunda WG, Carrano CJ.** 2009. Photolysis of iron-siderophore chelates promotes bacterial-algal mutualism. Proc. Natl. Acad. Sci. U. S. A. **106**:17071–17076.
38. **Bond DR, Strycharz-Glaven SM, Tender LM, Torres CI.** 2012. On electron transport through *Geobacter* biofilms. ChemSusChem **5**:1099–1105.
39. **Marshall CW, Ross DE, Fichot EB, Norman RS, May HD.** 2012. Electrosynthesis of commodity chemicals by an autotrophic microbial community. Appl. Environ. Microbiol. **78**:8412–8420.

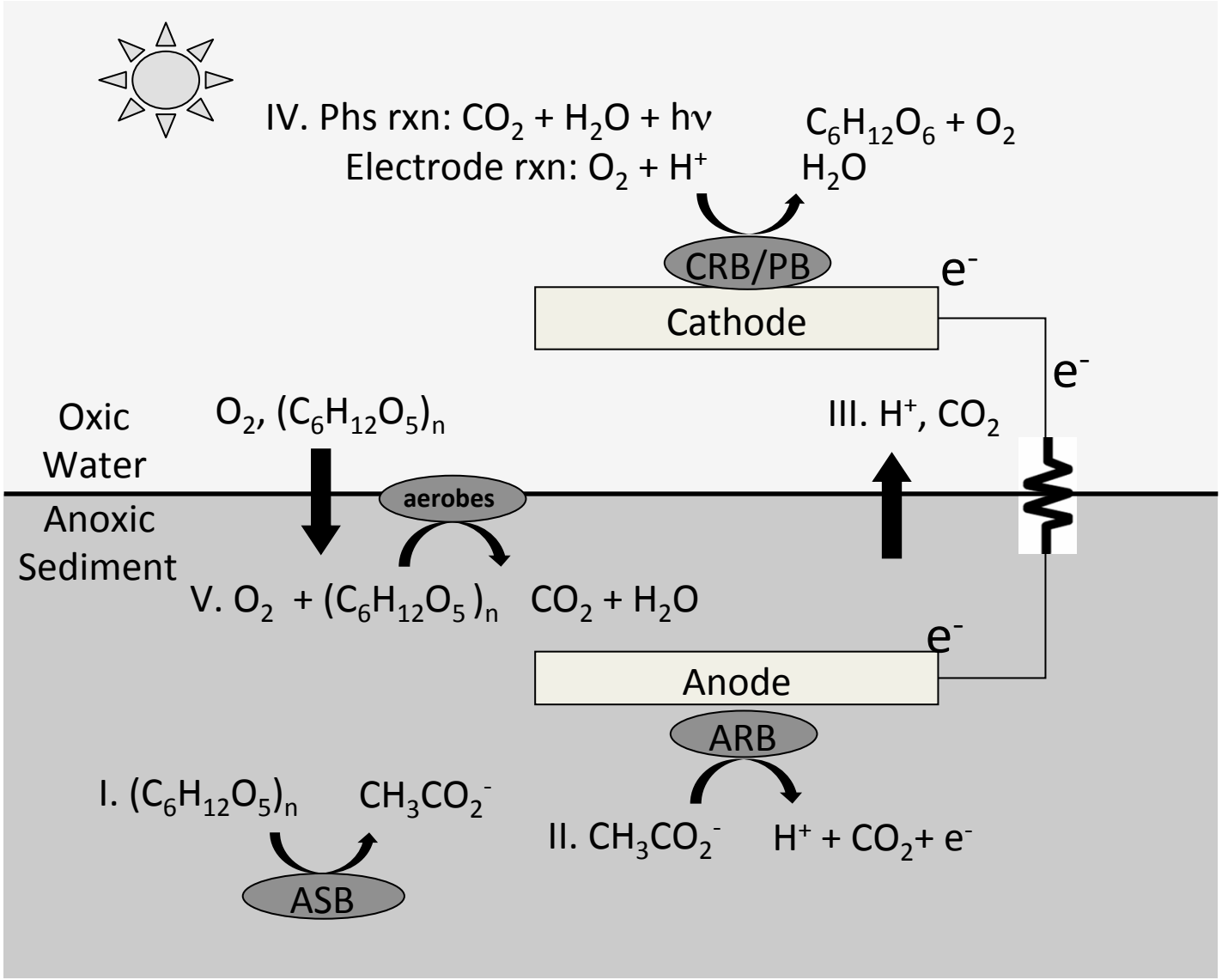

Figure S1 – General scheme for a sediment/seawater-based microbial solar cell (MSC). I. Complex organic matter in the sediment is converted to more simple compounds, such as acetate, by anaerobic sediment bacteria (ASB). II. Acetate is oxidized by anode respiring bacteria (ARB) which generates protons, carbon dioxide, and electrons. III. Protons and carbon dioxide diffuse through the sediment into the overlying seawater; electrons flow through the electrode circuit to the cathode. IV. Photosynthetic bacteria (PB) in the cathode biofilm convert carbon dioxide and water to glucose and oxygen using sunlight; oxygen is reduced to water by cathode respiring bacteria (CRB) catalyzing cathode oxidation. V. Oxygen and complex organic compounds produced during photosynthesis are consumed by aerobic bacteria residing on the sediment surface, while some complex organic matter is reintroduced into the sediment beginning the cycle again.

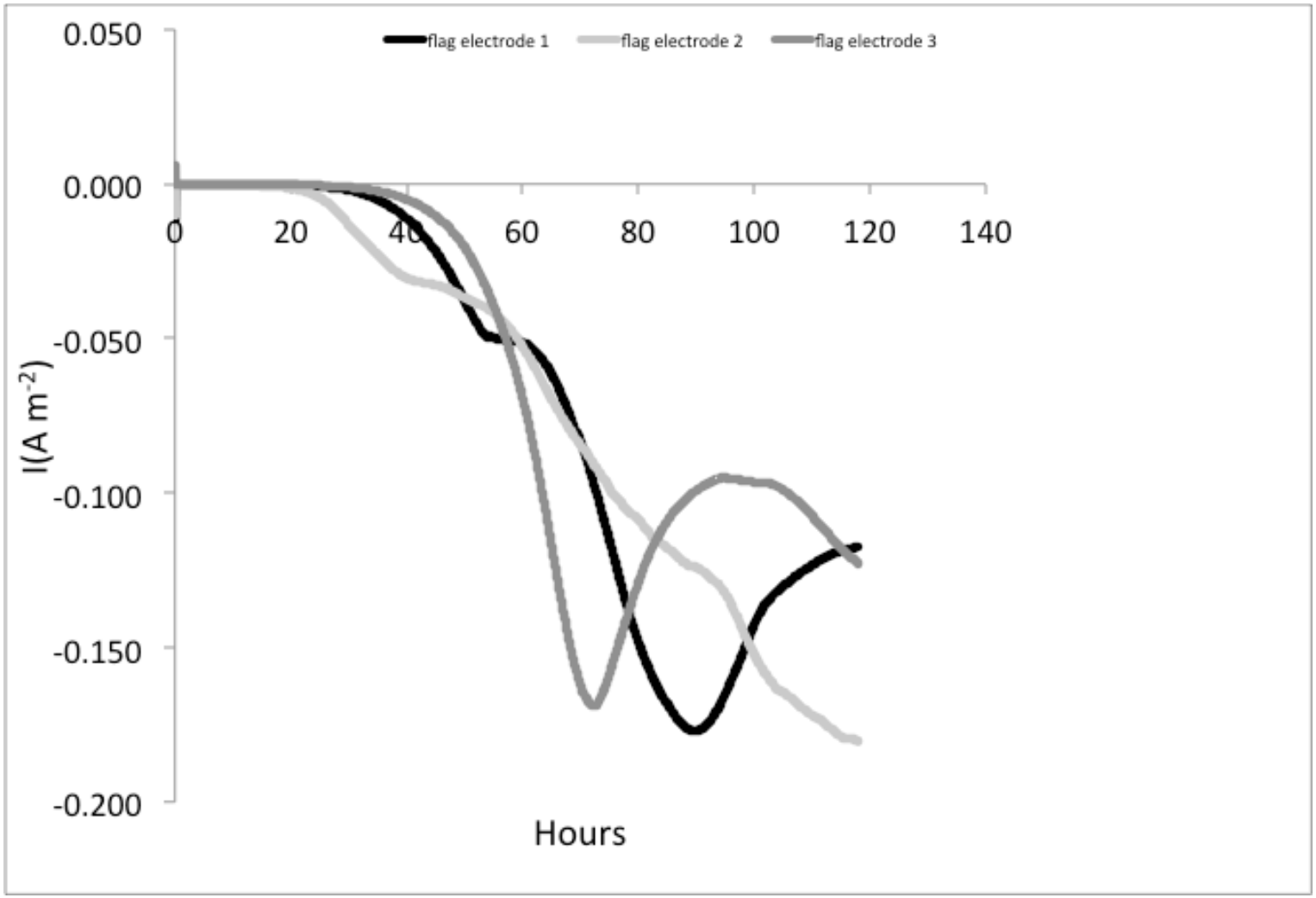

Figure S2 – Chronoamperometry recorded during growth of dark MSC enrichments in three electrode configuration on graphite flag electrodes for confocal laser scanning microscopy (CLSM).

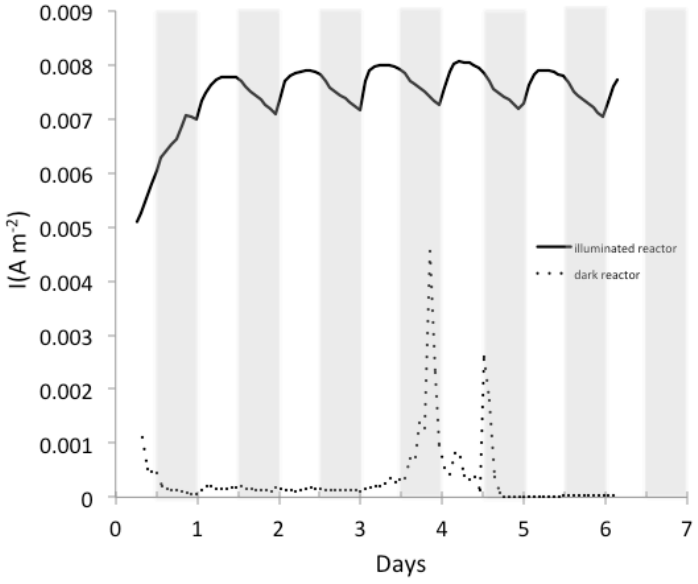

Figure S3 A – Day 0 represents time of discharge across a 5 kΩ resistor. Prior to discharge, reactors were left at open circuit for three days where the illuminated reactor was exposed to a 12 hour on/off light cycle and the dark reactor was maintained in darkness. The illuminated reactor quickly established a current associated with a diurnal light pattern, while only a small current was observed in the dark reactor.

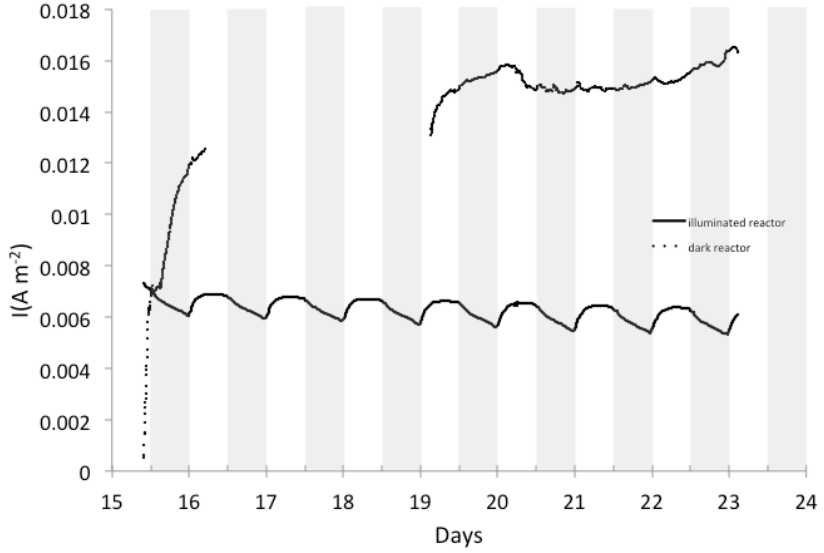

Figure S3 B – This plot is a continuation of the plot in Figure S3 A. Current increased in the dark MSC two weeks after discharge across a 5 kΩ resistor.

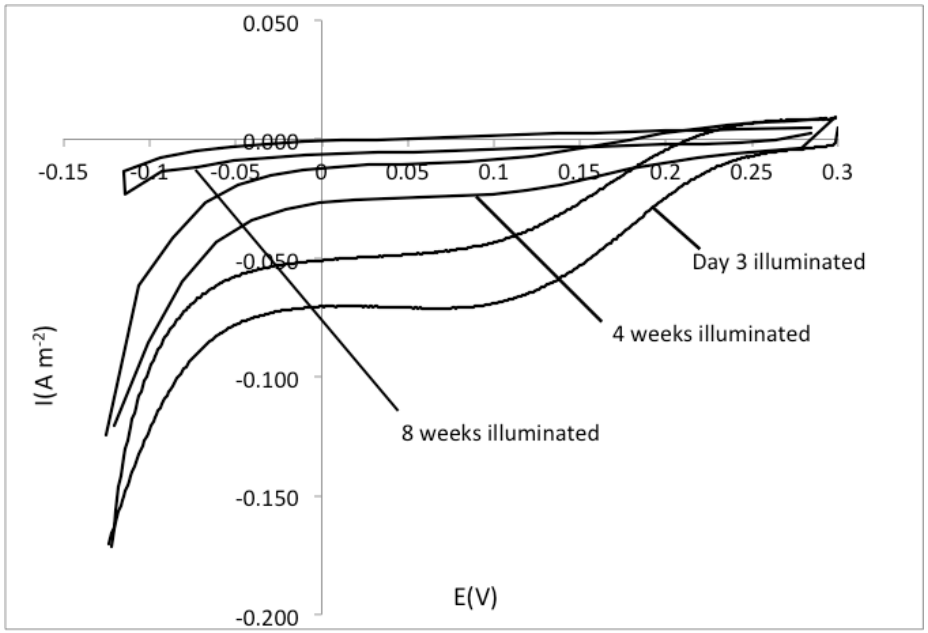

Figure S4A – Slow scan CV (0.0002 V/sec) of the illuminated microbial solar cell starting at Day 3 following discharge across a 5 kΩ resistor once a stable cell current was observed.

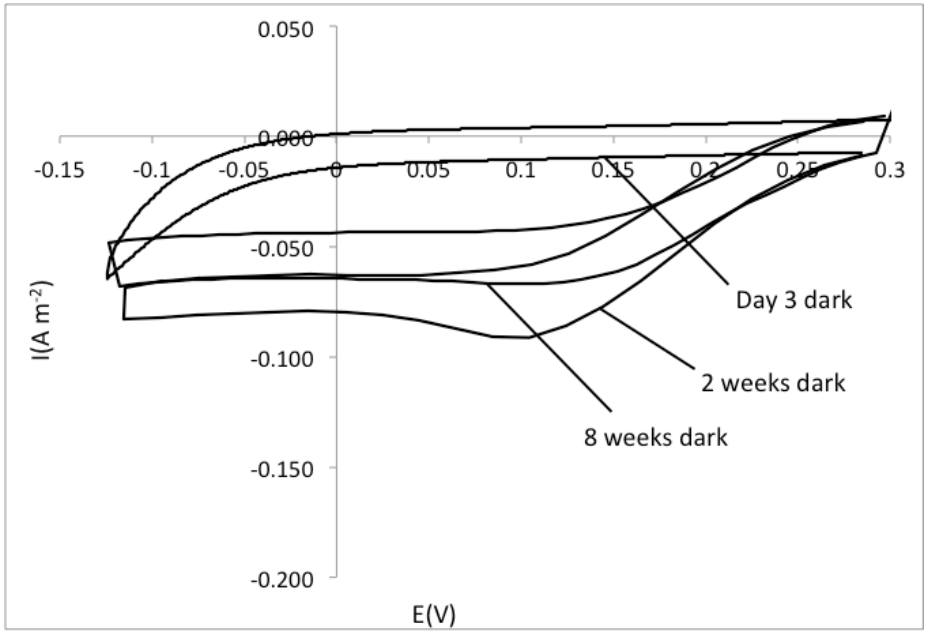

Figure S4B – Slow scan CV (0.0002 V/sec) of the dark microbial solar cell starting at Day 3 following discharge across a 5 kΩ resistor once a stable cell current was observed.

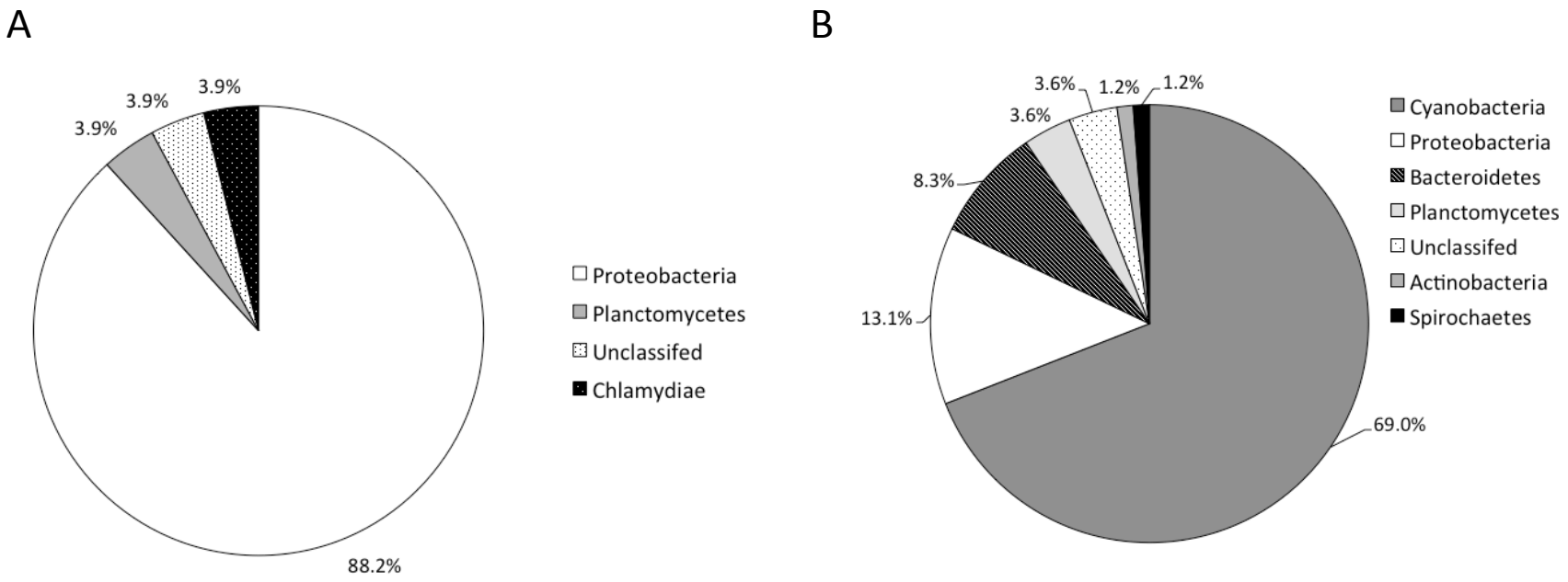

Figure S5 A&B –16S rRNA gene clone library composition from biocathode biofilms of the dark reactor (A) and the illuminated reactor (B). 16S rRNA gene clone libraries were generated from biofilm scrapings after 10 weeks at the stable cell current for each reactor.